TrwD, the Hexameric Traffic ATPase Encoded by Plasmid R388, Induces Membrane Destabilization and Hemifusion of Lipid Vesicles

Cristina Machón,[1,2] Susana Rivas,[1,2] Armando Albert,[3] Félix M. Goñi,[1]* and Fernando de la Cruz[2]

Unidad de Biofísica (CSIC-UPV/EHU) and Departamento de Bioquímica, Universidad del País Vasco, 48080 Bilbao,[1] Departamento de Biología Molecular (Unidad Asociada al CIB, CSIC), Universidad de Cantabria, 39011 Santander,[2] and Grupo de Cristalografía Macromolecular y Biología Estructural, Instituto de Química Física Rocasolano, CSIC, E-28006 Madrid,[3] Spain

TrwD, a hexameric ATP hydrolase encoded by plasmid R388, is a member of the PulE/VirB11 protein superfamily of traffic ATPases. It is essential for plasmid conjugation, particularly for expression of the conjugative W pilus. In the present study, we analyzed the effects that TrwD produced on unilamellar vesicles consisting of cardiolipin and phosphatidylcholine in equimolar amounts. TrwD induced dose-dependent vesicle aggregation and intervesicular mixing of the lipids located in the outer monolayers in the presence of calcium. It also induced extensive leakage of the vesicular aqueous contents. A point mutant of TrwD with a mutation in the P loop of the nucleotide-binding region (K203Q) that lacks both ATPase activity and the ability to support conjugation showed the same behavior as native TrwD in all of these processes, which were independent of the presence of ATP. Structure prediction methods revealed a close similarity to *Helicobacter pylori* protein HP0525, another member of the PulE/VirB11 family, whose crystal structure is known. The interpretation of our data in the light of this structure is that TrwD interacts with the lipid bilayer through hydrophobic regions in its N-terminal domain, which leads to a certain degree of membrane destabilization. TrwD appears to be a part of the conjugation machinery that interacts with the membranous systems in order to facilitate DNA transfer in bacteria.

The biological importance and evolutionary implications of bacterial conjugation are well known. This DNA transfer process occurs through a complex multistep mechanism involving the formation of various supramolecular assemblies. At least 15 different proteins are involved, and several of them are members of families implicated in bacterial conjugation or related processes (12, 19, 45). The TrwD-like protein family includes members involved in various instances of macromolecular transport in bacteria besides conjugation (18, 33). VirB11, a close relative of the family, is required for T-DNA transport from *Agrobacterium tumefaciens* into plant cells (39). PulE, a more remotely related homolog, is required for pullulanase secretion in *Klebsiella oxytoca* (34).

TrwD, also a member of the VirB11 family, is encoded by conjugative plasmid R388. This plasmid contains one of the simplest gene organizations known for a conjugative transfer system (8). The *trwD* gene is located in PIL$_W$, the R388 region involved in pilus formation. Many TrwD homologues are known (35), and many have functions unrelated to conjugation. TrwD was cloned and purified by us as a glutathione *S*-transferase (GST)–TrwD fusion protein (35). The fusion protein was functionally active, as shown by genetic complementation assays. It displayed ATP hydrolase activity that was essential for R388 conjugation. When the conserved lysine residue of the nucleotide-binding site (Walker box) of TrwD was replaced with glutamine, the mutant form (K203Q) lacked

ATPase activity and had a dominant negative effect on conjugation, suggesting that the mutation did not abolish the capacity of TrwD to interact with other components of the conjugative machinery (35). Recent work has shown that TrwD, together with other members of the VirB11 family, gives rise to hexameric ring structures (21, 22)

Several observations point toward an interaction of TrwD with bacterial membranes, namely, (i) the fact that the purification yield increased in the presence of 0.5 M NaCl, as is often the case with peripheral membrane proteins; (ii) TrwD was found to be at least partially associated with the bacterial outer membrane; and (iii) the ATPase activity of TrwD increased in the presence of mixed micelles of detergent and phospholipids (35). In view of these data, an investigation was undertaken to explore specifically the interaction of TrwD with membranes. With this purpose, native and mutant (K203Q) forms of TrwD were prepared as described previously (35). Small unilamellar vesicles (SUV) and large unilamellar vesicles (LUV) with defined lipid compositions were used as model membranes. Results showed that, under our conditions, TrwD induced vesicle aggregation with leakage of vesicular aqueous contents and intervesicular lipid mixing but no intervesicular mixing of aqueous contents (fusion). Recently, Yeo et al. (44) have reported the crystal structure of protein HP0525, another member of the TrwD family whose conformation shows close similarities to the predicted secondary structure of TrwD. Yeo et al. (44) showed that the N-terminal domain of the protein contains a hydrophobic surface and suggested that this region of the protein is responsible for membrane association. We suggest that the membrane-active character of TrwD, shown by the exper-

* Corresponding author. Mailing address: Unidad de Biofísica (CSIC-UPV/EHU) and Departamento de Bioquímica, Universidad del País Vasco, Aptdo. 644, 48080 Bilbao, Spain. Phone: 34-946012542. Fax: 34-944648500. E-mail: gbpgourf@lg.ehu.es.

iments presented in this work, is caused by a similar hydrophobic region in our protein.

MATERIALS AND METHODS

TrwD was purified in the form of a fusion protein with GST from soluble extracts of *Escherichia coli* D1210 containing plasmid pSU4618 as described by Rivas et al. (35). When required, the fusion protein was incubated with factor Xa and the fragment corresponding to TrwD was purified by affinity chromatography as described previously. A site-specific mutant form of TrwD, namely, K203Q, was purified from *E. coli* D1210 containing plasmid pSU4631 by the same procedure as used for the native protein, as described in our previous work.

Egg phosphatidylcholine (PC) and egg phosphatidylglycerol (PG) were grade I from Lipid Products (South Nutfield, United Kingdom). Cardiolipin (CL), cholesterol (Ch), and Triton X-100 were purchased from Sigma. Egg sphingomyelin was from Avanti Polar Lipids (Alabaster, Ala.). 1-Aminonaphthalene-1,3,6-trisulfonic acid (ANTS), *p*-xylenebis(pyridinium bromide) (DPX), and octadecylrhodamine B (R18) were supplied by Molecular Probes, Inc. (Eugene, Oreg.). *N*-(7-Nitro-2,1,3-benzoxadiazol-4-yl) (NBD)-phosphatidylethanolamine (PE) and *N*-(lissamine rhodamine B-sulfonyl)-dioleoyl PE (rhodamine-PE) were obtained from Avanti. The lipids were mixed in organic solvent, evaporated thoroughly under a stream of N_2, and left under a vacuum for at least 2 h to remove traces of solvent. The dry lipid film was then dispersed in the appropriate aqueous solution. SUV were prepared by sonication with an MSE (Crawley) probe (10- to 12-μm amplitude) for 40 min at 4°C (1). Vesicle size was measured by quasielastic light scattering (QELS) in a Malvern Zetasizer 4 spectrometer. For QELS measurements, the buffer had been previously filtered through 0.22-μm-pore-size filters. The average diameter of the vesicles was 45 to 55 nm.

LUV were prepared by the extrusion method of Mayer et al. (24) using Nuclepore filters with a 0.1-μm pore diameter at room temperature. QELS measurements revealed an average diameter of 110 to 120 nm for these large vesicles.

Destabilization of vesicle bilayers by TrwD. To monitor the interaction of TrwD with model membranes, fluorescence measurements were done with a Shimadzu RF-540 spectrofluorometer. Samples containing a 0.2 mM lipid concentration in the form of vesicles were used; the process was initiated by addition of TrwD protein (concentration, 17 nM) to a protein-lipid ratio of 1:12,000. Samples were continuously stirred. The buffer contained 50 mM Tris-HCl (pH 7.5), 100 mM NaCl, and 10 mM $CaCl_2$ unless otherwise stated. All experiments were done at 25°C.

Vesicle aggregation assays. Vesicle aggregation was estimated as an increase in the amount of light scattered by the suspension with both the excitation and emission monochromators of the spectrofluorometer at 520 nm.

Lipid mixing. Lipid mixing was measured by dilution in the bilayer of self-quenching probe R18 as described by Hoekstra et al. (20). The 0% fluorescence level (or 0% mixing) was determined from a 1:4 mixture of 8 mol% R18 containing liposomes and R18-free liposomes. The fluorescence of the same amount of liposomes with the diluted probe uniformly distributed, i.e., 1.6 mol% R18-containing liposomes, was taken as the 100% fluorescence level or 100% lipid mixing.

Alternatively, lipid mixing was assayed by the resonance energy method of Struck et al. (40) using NBD-PE and rhodamine-PE. A modification of the latter method, proposed by McIntyre and Sleight (25), was used to measure the mixing of inner monolayer lipids. In this procedure, vesicles containing NBD-PE and rhodamine-PE are treated with sodium dithionite so that the fluorophores are reduced and their fluorescence is quenched. Since the bilayer is relatively impermeable to dithionite, the fluorophores located in the inner monolayer remain unquenched and most of the signal arises from fluorescence probes in the inner monolayer. Excess dithionite is then removed by passing the vesicle suspension through a Sephadex G-75 column. TrwD-induced lipid mixing in these vesicles actually reports on the intermixing of inner vesicle monolayers.

Mixing and release of aqueous contents. Mixing of vesicle aqueous contents and vesicle leakage were estimated by using the ANTS/DPX fluorescent probe system described by Ellens et al. (15). The osmolality of intra- and extravesicular solutions was measured in a cryoscopic osmometer (Osmomat 030; Gonotec, Berlin, Germany) and adjusted to 0.3 osmol/kg by addition of NaCl. Fluorescence scales were calibrated for fusion and release assays as described previously (28). The excitation wavelength was adjusted to 355 nm. An interference filter (470 nm) was used to avoid scattered excitation light.

Protein binding to vesicles. To measure the parameters of TrwD binding to membranes, 0.5 mM LUV in D_2O-buffer (50 mM Tris-HCl [pH 7.5] and 100 mM NaCl in D_2O) were incubated with protein (0.1 to 1.0 μM in D_2O-buffer) and centrifuged at 513,000 × *g* under conditions leading to vesicle flotation, as

described by Pereira et al. (32). Protein concentrations in appropriate samples were determined by comparison with known amounts of TrwD in Coomassie blue-stained gels after sodium dodecyl sulfate-polyacrylamide gel electrophoresis. Bands were quantified by using the Quantity One software in a Fluor-S MultiImager (Bio-Rad). Lipid concentration was determined by using the fluorescent probe rhodamine-PE mentioned above.

RESULTS

Preliminary experiments were done with SUV with the following compositions: (i) PC-PE-Ch at a 2:1:1 molar ratio, (ii) sphingomyelin-PE-Ch at a 2:1:1 ratio, (iii) PC-PG at a 1:1 ratio, and (d) PC-CL at a 1:1 ratio. These compositions were chosen for their different physical properties and are not typical of bacterial membranes. The following buffers were used: (i) 50 mM Tris-HCl (pH 7.5), (ii) 5 mM $MgCl_2$–50 mM Tris-HCl (pH 7.5), and (iii) 150 mM NaCl–50 mM Tris-HCl (pH 7.5). In all cases, TrwD-induced vesicle aggregation was detected by measuring changes in light scattering of the liposomal suspension. Only in the case of CL-containing bilayers and magnesium-containing buffer was aggregation observed. All subsequent experiments were done with PC-CL (1:1 molar ratio) bilayers in the presence of divalent cations. This system has some tendency to aggregate, even in the absence of TrwD (42, 43), so that a small proportion (usually less than 10%) of the aggregation signal detected in the presence of TrwD could be due to spontaneous vesicle aggregation (see specific examples below). To correct for this, all of the results shown were corrected for the changes observed in the absence of protein. Unless otherwise stated, the total lipid concentration in the assay was 0.2 mM. TrwD, in the form of a fusion protein with GST, was usually added at 17 nM.

Studies with sonicated SUV. Divalent cations often play a substantial role in macromolecular assemblies and in membrane processes. Since Mg^{2+} was seen to facilitate aggregation in the preliminary experiments described above, the effects of various concentrations of Mg^{2+} and Ca^{2+} on TrwD-induced vesicle aggregation were tested (Fig. 1). In general, Ca^{2+} was more potent than Mg^{2+} in facilitating aggregation (note the different ordinate scales in Fig. 1A and B). Consequently, all further experiments, unless otherwise stated, were done with 10 mM $CaCl_2$–100 mM NaCl–50 mM Tris-HCl (pH 7.5) buffer. When TrwD ATPase activity was tested, Mg^{2+} allowed higher activities than Ca^{2+}, as expected for an ATPase. This underlines the twofold activity of TrwD, as a membrane-active protein and as an ATPase.

A series of control experiments were performed in order to ensure that the observed effects were due to a specific effect of TrwD in its native conformation. Although GST-TrwD was used in most experiments, free TrwD was occasionally prepared by factor Xa hydrolysis of the fusion protein (35). Free TrwD had the same effects as GST-TrwD, at equal concentrations, on vesicle aggregation. Conversely, addition of bovine serum albumin, at concentrations 1×, 10×, and 100× that of TrwD, had no effect on vesicle aggregation. Similar experiments with GST produced no effect. Similarly, no effect was observed when TrwD denatured by repeated freezing and thawing or by heating at 100°C for 30 min, was added to the SUV suspension in the presence of 10 mM Ca^{2+}.

TrwD-elicited vesicle aggregation was dose dependent, as shown in Fig. 2, and the slope of the aggregation-versus-time
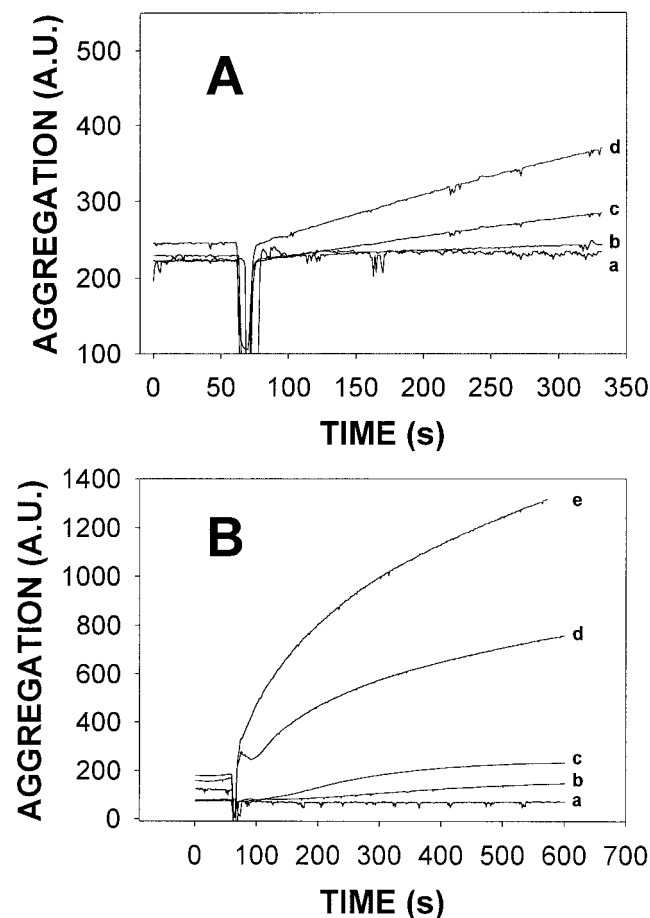
FIG. 1. Influence of divalent cations on TrwD-induced aggregation of SUV composed of PC-CL at an equimolar ratio. Vesicle aggregation was assayed as an increase in light scattering (520 nm) by the suspension. SUV were suspended in 100 mM NaCl–50 mM Tris-HCl buffer (pH 7.5) with additions as follows: A, MgCl; B, CaCl$_2$. Curves: a, 0 mM; b, 1 mM; c, 2.5 mM; d, 5 mM; e, 10 mM. Protein was added at 60 s.
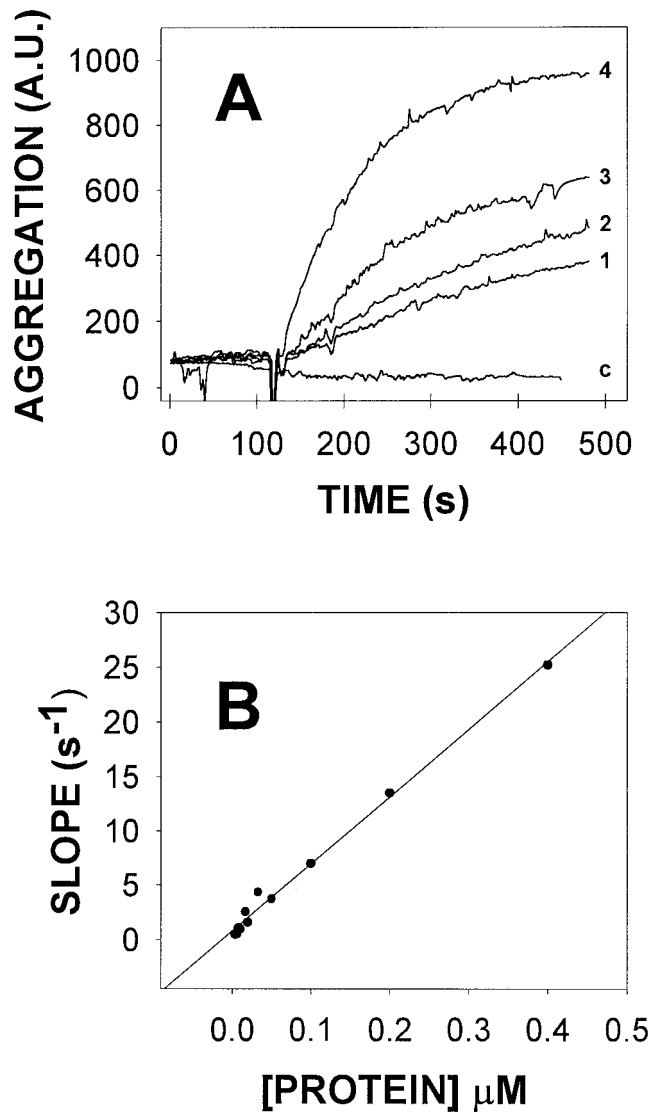

FIG. 2. Dose dependence of SUV aggregation induced by TrwD. (A) Selected examples: curves 1 to 4 correspond to experiments in which protein concentrations were, respectively, 8, 17, 20, and 100 nM. Curve c corresponds to a control experiment in which the protein (100 nM) had been heat denatured prior to its addition to the vesicle suspension. (B) Initial slopes of the scattering-versus-time curves plotted as a function of the TrwD concentration. A.U., arbitrary units.

curves increased linearly between 4 and 400 nM protein at a constant vesicle concentration.

Protein-induced vesicle aggregation is often accompanied by other membrane-dependent phenomena, e.g., intervesicular lipid mixing, leakage of aqueous contents, or mixing of vesicular aqueous contents (18, 23, 30). These phenomena were independently tested in our system. As seen in Fig. 3, under the same conditions leading to vesicle aggregation, TrwD induced intervesicular lipid mixing and extensive release of aqueous contents. However, no mixing of vesicular aqueous contents was detected (Fig. 3, curve d). Usually, intervesicular mixing of both bilayer lipids and aqueous contents is required to ascertain the fusion of vesicles (6). In a situation such as that shown in Fig. 3, the extensive leakage may obscure the result of contents mixing but the fact that lipid mixing did not go beyond 40% speaks against the presence of vesicle fusion induced by TrwD, because such a value may reflect the mixing of just external monolayer lipids. Thus, the data in Fig. 1 to 3 are best interpreted as TrwD specifically inducing SUV aggregation,

vesicle leakage, and intervesicular lipid mixing but no vesicle-vesicle fusion.

Studies with LUV. SUV, usually obtained by sonication, have an inherent metastability derived from their small radius or high curvature (2, 16). This property makes them ideal for the detection of small perturbations caused by proteins or other agents. However, the curvature of cell membranes is better represented by large liposomes. Therefore, the results obtained with SUV were complemented with studies using LUV as model membranes. In the latter experiments, a mutant protein (K203Q) was also studied in which a conserved lysine residue in the nucleotide-binding site was replaced with glutamine, with which the ATPase activity is lost (35).
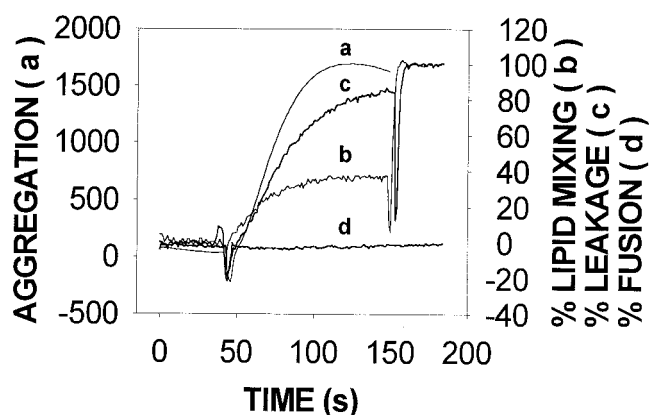
FIG. 3. Effects of TrwD on SUV stability. Curve a shows vesicle aggregation, which was assayed as an increase in light scattering (520 nm) by the suspension. Curve b shows intervesicular lipid mixing, which was measured by dilution in the bilayer of self-quenching probe R18. The excitation and emission wavelengths were, respectively, 560 and 590 nm. Curve c shows release of vesicular aqueous contents, which was estimated with the ANTS/DPX fluorescent probe system. The excitation and emission wavelengths were, respectively, 355 and 520 nm. Curve d shows intervesicular mixing of aqueous contents, which was also measured with the ANTS/DPX system. In all cases, SUV composed of PC-CL at a 1:1 molar ratio were used. Phospholipid and protein concentrations were, respectively, 0.2 mM and 17 nM.

TrwD induced aggregation of LUV composed of PC-CL at a 1:1 molar ratio (Fig. 4A). The relative increase in turbidity was smaller than that obtained with SUV (compare with the data in Fig. 3). This could be due to a variety of reasons, chief among them the larger basal turbidity of LUV suspensions and the larger size, and thus the smaller diffusion coefficient, of LUV. Both of these reasons also explain why aggregation of LUV occurs at a much lower rate than that of SUV (compare Fig. 3 and 4A). The K203Q mutant was indistinguishable from the native protein in its vesicle-aggregating properties. Vesicle aggregation induced by TrwD in the presence of 3 mM Mg^{2+}-ATP gave exactly the same results as shown in Fig. 4A in the absence of nucleotide.

Intervesicular lipid mixing was also induced by TrwD in LUV preparations, as shown in Fig. 4B. Lipid mixing occurred to a lesser extent and at a slower rate than that of SUV (compare with Fig. 3). This was to be expected from the relatively reduced rate and extent of LUV aggregation, since aggregation is an obvious prerequisite for significant lipid mixing to occur. Again, the K203Q mutant behaved in a manner similar to that of native TrwD.

As mentioned above, PC-CL vesicles have a spontaneous tendency to aggregate; therefore, the results shown in Fig. 4 correspond to the TrwD-induced spectroscopic signal after subtraction of the spontaneous signal. This is explicitly shown in Fig. 5 for a representative example.

The lipid mixing results shown in Fig. 3 and 4B were obtained with the R18 assay (20). However, this lipid has some tendency to partition into the aqueous medium, thus giving rise to possible artifacts (38). For this reason, the lipid mixing test was repeated with a method based on fluorescence energy transfer between NBD-PE and rhodamine-PE (40). Very similar results were obtained: 23% lipid mixing after 6.0 min with
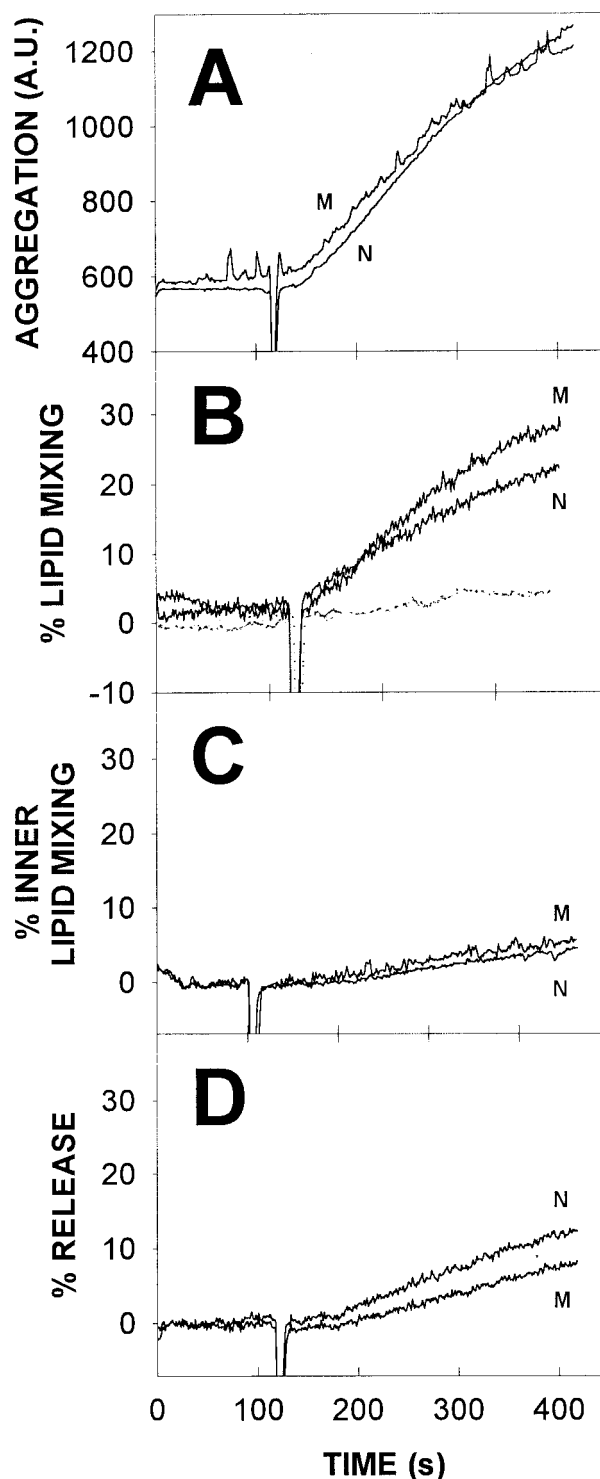

FIG. 4. Effects of TrwD on LUV stability. (A) Vesicle aggregation measured as light scattering (520 nm). (B) Intervesicular lipid mixing measured by the R18 method (continuous line) and intervesicular mixing of aqueous contents (dotted line) measured as described in the legend to Fig. 3C. (C) Intervesicular mixing of inner monolayer lipids measured as described by McIntyre and Sleight (25) with NBD-PE and rhodamine-PE. (D) Release of vesicular aqueous contents measured as described in the legend to Fig. 3. Phospholipid and protein concentrations were as described in the legend to Fig. 3. N and M refer to the native and mutant forms of TrwD, respectively.
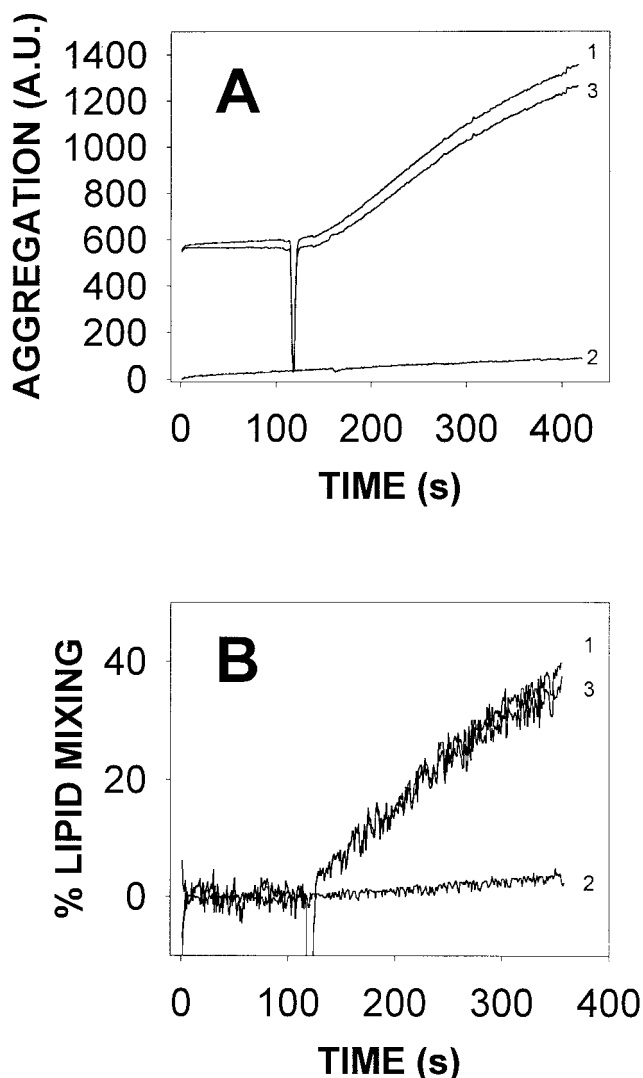
FIG. 5. Influence of spontaneous aggregation and lipid mixing in LUV consisting of CL-PC at a 1:1 ratio. The lipid concentration was 0.2 mM. Panels: A, vesicle aggregation; B, intervesicular lipid mixing. Curves: 1, experimentally observed effect upon addition of 17 nM TrwD; 2, experimentally observed effect upon mixing of the vesicles with a buffer containing 10 mM calcium in the absence of protein; 3, difference (curve 1 minus curve 2). Curve 3 is an example of the corrected signals depicted in Fig. 1 to 4. A.U., arbitrary units.

R18 versus 18% with NBD-PE/rhodamine-PE (data not shown), thus confirming the previous observations. With the NBD-PE/rhodamine-PE system, the K203Q mutant behaved like native TrwD.

The NBD-PE/rhodamine-PE method has the advantage that it can be modified to reveal specifically the intermixing of lipids in the inner monolayer of the vesicles. This is achieved by reducing with sodium dithionite the fluorescent probes in the outer monolayer, thus quenching their fluorescence. Excess dithionite is then removed with a Sephadex G-75 column (25). Mixing of inner monolayers should normally occur when complete vesicle fusion (i.e., mixing of lipids and contents) is taking place. As seen in Fig. 4C, no significant mixing of inner mono-layer lipids was elicited by the native or mutant form of TrwD.

In agreement with these observations, intervesicular mixing of aqueous contents failed to occur to any significant extent (Fig. 4B, dotted line), thus confirming the absence of vesicle fusion.

Finally, leakage of aqueous contents from LUV was also studied. TrwD induced release of vesicular contents (Fig. 4D) but to a much smaller extent than in the case of SUV. This is a case in which the metastable character of SUV led to a response different from that produced by the more stable LUV, as will be discussed below.

In summary, TrwD specifically induced vesicle aggregation, intervesicular lipid mixing, and release of aqueous vesicular contents but not complete vesicle fusion. Very similar results were obtained with SUV and LUV, the differences observed between the two systems being due mainly to the inherent properties of the respective bilayers. The mechanism by which TrwD produced these effects is independent from its ATP hydrolase activity and may be related to the presence of ex-posed hydrophobic regions in the protein, as proposed below.

TrwD binding to LUV. In order to quantify TrwD binding to membranes, LUV were mixed with the protein in D_2O-buffer and centrifuged at high speed under conditions leading to vesicle flotation as described by Pereira et al. (31, 32). Vesicle-bound and free proteins are expected to separate under these conditions. For total TrwD concentrations ranging from 0.1 to 1.0 μM, 45% ± 15% (n = 8) of the total protein became incorporated into the liposome fraction, remaining in the up-per fraction of the tube, while the free protein sedimented at the bottom. (Fig. 6). This is in agreement with the previous finding that the protein is found partly free and partly mem-brane bound in the cell (35).

DISCUSSION

TrwD displays two different activities, that of an ATP hy-drolase (35) and that of a protein that interacts with and perturbs the stability of membranes (this paper). The results in Fig. 4, which show no difference in membrane activity between native TrwD and a mutant form inactive in ATP hydrolysis, indicate that the two activities need not be coupled in the mechanism of TrwD function. Moreover, the dominant char-acter of the K203Q mutation (35) suggests that the mutant form kept intact its capacity to form hexamers. The same is true for the TrwD homolog TrbB. The equivalent mutant form of this protein (K161A) was shown to be Tra⁻, transdominant, and still capable of assembling into hexamers (22)

TrwD-induced membrane perturbation. The precise effect of TrwD on bilayer architecture is defined by the experiments in Fig. 2 to 4. The protein induces vesicle aggregation in a dose-dependent way. Aggregation usually occurs as a mecha-nism by which to avoid contacts between water and hydropho-bic molecules. This is, e.g., the mechanism of liposome aggre-gation due to the in situ production of diacylglycerol by phospholipase C (4). In the present case, TrwD binding to (and perhaps partial insertion into [see below]) the lipid bilayer may lead to exposure of the membrane hydrophobic matrix. Alter-natively, the protein may expose additional hydrophobic areas on its surface upon binding of the bilayer. Any of these phe-nomena would explain the observed aggregation.

Leakage of vesicular contents occurs concomitantly with ag-gregation. Leakage is more extensive in SUV, and it probably
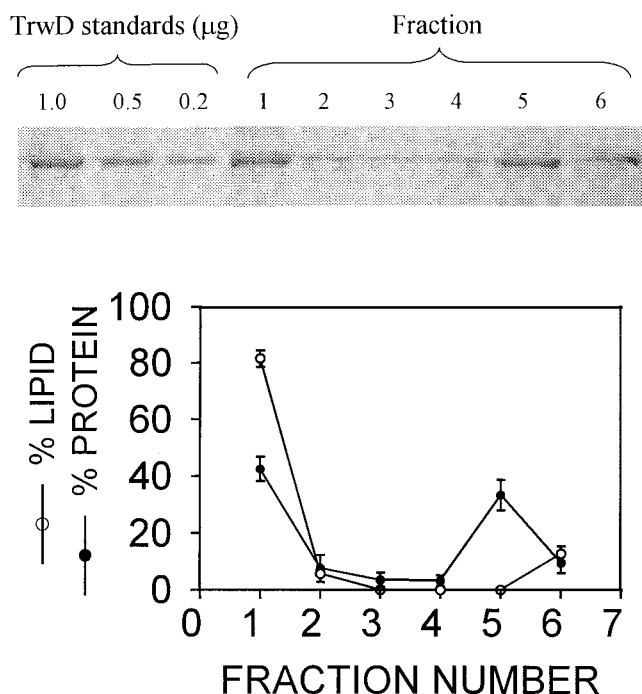
FIG. 6. Ultracentrifugation experiment to demonstrate protein incorporation into liposomes. TrwD at 0.7 μM was incubated with 0.5 mM LUV composed of PC-CL at a 1:1 ratio in D_2O-buffer for 15 min. The sample was ultracentrifuged at 513,000 × g, and 200-μl fractions were collected (1 [top] to 5 [bottom]). A 200-μl volume of extra buffer was added to the tube to resuspend any remaining protein and lipid (fraction 6). TrwD concentration was determined after sodium dodecyl sulfate-polyacrylamide gel electrophoresis by comparison with known standards, as shown at the top. The lipid concentration was determined by measuring the fluorescence signal of rhodamine-PE. The graph at the bottom shows the results (average ± the standard error of the mean) of eight experiments with total TrwD concentrations in the 0.1- to 1.0-μM range.

occurs by a different mechanism in the small and large molecules. In the latter, partial leakage is probably a mere consequence of the lipid rearrangements secondary to protein insertion, as occurs with magainins (23) or with *E. coli* α-hemolysin (37). In SUV, however, because of their lateral tension, protein insertion probably leads to opening up of the vesicle, which behaves like a punctured balloon, so that vesicular contents are rapidly released. The remnants of the bilayer then reassemble into a new vesicle. This mechanism of lysis and reassembly has been shown to operate for surfactants acting on SUV (1, 14), and it may work as well for amphiphilic protein domains.

A third effect of TrwD on liposomes is to induce intervesicular lipid mixing. This phenomenon requires an intimate degree of contact between vesicles, beyond the mere aggregation, that excludes water molecules from the vesicle contact area (6). In our case, the data from SUV and LUV concur in presenting a phenomenon of lipid mixing that never goes beyond 50% of the total lipid. In addition, it is limited to the outer monolayer (Fig. 4C) and is not accompanied by mixing of aqueous contents (Fig. 3 and 4B). Hence, TrwD appears to induce a phenomenon that has been called hemifusion (10) or close apposition (41) of vesicles, i.e., mixing of outer lipid monolayers but not the inner compartments.

The nature of TrwD-bilayer interaction. Although the required presence of a negatively charged lipid may speak in favor of electrostatic binding of TrwD to the membrane, the concomitant demand of Ca^{2+} at millimolar concentrations (i.e., 1 order of magnitude above the lipid concentration) suggests, instead, that the lipid is electrically neutralized by Ca^{2+} so that the relative weight of any electrostatic component in protein binding must be small. Rather, a combination of divalent cation and negative divalent CL suggests the lateral separation of CL-Ca^{2+} complexes into separate domains in the plane of the membrane. CL has been shown to increase the ATPase activity in TrwD (35) and induce conformational changes (detected through changes in intrinsic fluorescence) in closely related members of the TrwD family (22).

In-plane formation of lipid domains is expected for the CL-Ca^{2+} system (27) but not for bilayers based on PG, which was less active than CL in supporting TrwD-induced vesicle aggregation. Interdomain interfaces are known to facilitate insertion into membranes, as shown for gramicidin A (13), *E. coli* α-hemolysin (3), or protein kinase C (17). Thus, formation of separate domains can also favor the interaction of TrwD with the lipid bilayer.

Yeo et al. (44) have elucidated the crystal structure of hexameric HP0525 from *Helicobacter pylori*, which is another member of the VirB11 family and is related to TrwD. The predicted secondary structure of TrwD for the N-terminal domain (Fig. 7) is the same as the calculated structure for HP0525 (44). It is thus reasonable to assume that the two proteins have the same overall folding pattern in this region, including membrane binding through the N-terminal domain. Electron microscopic studies reveal that they both display the same low-resolution quaternary structure (22). The molecular surface of HP0525 exhibits few hydrophobic regions, which are concentrated at the bottom of the hexamer, corresponding to α-helices A and B and to the loops connecting the latter with β-strands 3 and 4. Helices A and B are conserved in TrwD (Fig. 7). Helix A is amphipathic in both proteins. Helix B, however, is almost fully hydrophobic in TrwD while it is amphipathic in HP0525. These data and predictions lead us to postulate that TrwD interacts with the membrane bilayer, through the stretches designated helices A and B in Fig. 7, at the N-terminal domain of the protein.

Yeo et al. (44) have suggested that hexameric HP0525 spans the membrane and forms an ATP-dependent pore. In their view, the small hole formed by the pore in its closed form would be about 10 Å in diameter. However, a pore of this size would permit complete release of the vesicular aqueous contents in milliseconds (29). This is in contrast with the rather slow rates of leakage, compared to the rates of protein-induced vesicle aggregation, seen in Fig. 4. The fact that TrwD-induced leakage is ATP independent also speaks against the notion that the mechanism proposed by Yeo et al. (44) is applicable to TrwD. Moreover, a transmembrane protein pore, as proposed by those authors, would hardly be compatible with a lack of mixing of vesicle inner monolayers (Fig. 4C). In general, our data point more toward a kind of TrwD organization in the membrane that affects primarily the outer lipid monolayer in the vesicles.

Other water-soluble proteins are known that induce profound modifications in membrane lipid organization without

```
                        αA                              β1
HP0525  (1)  MTEDRLSAEDKKFLEVERALKEAAALNPLRHATEELFGDFLKMENITEICY
TrwD    (1)  -------MSTVSKASPLSSGNRVGKDQAVAQLLRPLDRFLDAPEVTELSI
                           αA1       αA2        β1

              β2        β3              αB
HP0525 (51)  NGNKVVWVLKNNGEWQPFDVRDRKAFSLSRLMHFARCCASFKKKTIDNYE
TrwD   (44)  CRPGEVWTKTFEG----WQVHEVPELTEPFLQALITAIIVYNG--V-A-P
              β2        β3              αB

           β4      β5              β6              αC
HP0525 (101) NPILSSNLANGERVQIVLSPVTVNDETISISIRIPSKTTYPHSFFEEQGF
TrwD    (86) KSVNYVVLPGGQRGTIAQAPAVIDGT-LSFLIRKHSLVVKTLEELDAEGA
                     β5              β6

                                              αD
HP0525 (151) YNLLDN-------------------------KE--------QAISAIK
TrwD   (135) FDTFTDVSFNKPSAEEANHYLTVQDFTRLEPFEVELLKLKRDGTIREFLE
                                          αD1       αD2

            αD    β7       αE              β8
HP0525 (166) DGIAIGKNVIVCGGTGSGKTTYIKSIMEFIPKEERIISIEDTEEIVFKHH
TrwD   (185) KCVLYKRNIIAGKTGSGKTTFARSLIEKVPPEERIITIEDVHELFLPNH
             αD2   β7       αE              β8a     β8b

            β9         αF       β10            αG
HP0525 (216) KNYTQLFFGGN---ITSADCLKSCLRMRPDRIILGELRSSEAYDFYNVLC
TrwD   (235) PNRVHMLYGYGAGRVSADECLAACMRQSPDRIFLAELRGNEAWEYLNSLN
             β9         αF       β10            αG

            β11      αH              αI
HP0525 (263) SGHKGTLTTTLHAGSSEEAFIRLANMSSSNSAARNIKFES-LIEGFKDLID
TrwD   (285) TGHPGSITTTHANNALQTFERCATLIKKSDVGRQLEME-MIKLVLYTTID
                      αH              αI      β12

            β12      β13
HP0525 (312) MIVHINHHKQCDEFYIKHR-------
TrwD   (334) VVLFFKDR-KLVEVFYDPIFSKSKMA
             β12      β13
```
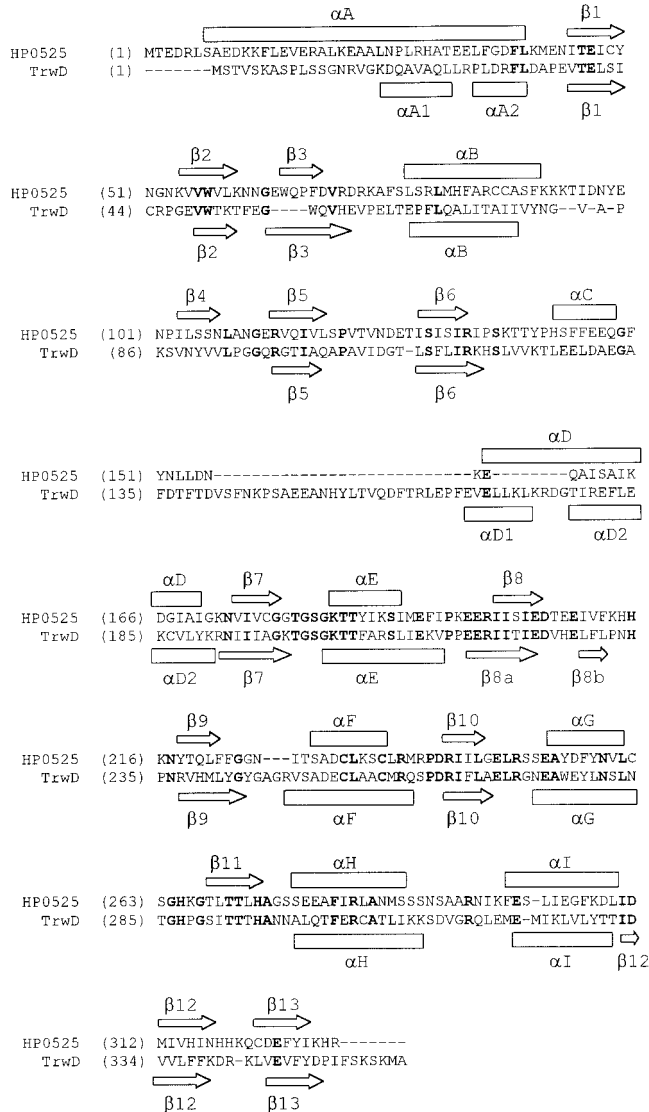
FIG. 7. Alignment of the amino acid sequences of proteins HP0525 (accession no. E64585) and TrwD (accession no. CAA57032). To construct this alignment, a set of 20 proteins were selected among the closest TrwD homologs, excluding nearly identical sequences, with BLAST scores of better than 10^{-20}. This set included HP0525 (P = 3 × 10^{-29}). The alignment was done by using the ClustalW algorithm (2), and the two relevant sequences were extracted from the alignment. Above the alignment is the allocation of the secondary-structure elements of HP0525 according to its three-dimensional structure (43). Below the alignment is the secondary-structure prediction for TrwD, which was calculated from the multiple alignment described above by the PHD program (36). α-Helices and β-sheets are shown where PHD gave reliabilities of >82%. Amino acids invariant between the two proteins are in bold.

becoming strongly bound to the bilayer. Glyceraldehyde-3-phosphate dehydrogenase, a soluble protein containing hydrophobic patches on the molecular surface, has been reported to destabilize and fuse SUV under certain conditions (26). A variety of amphipathic peptides act in a similar way (5, 9, 23, 30). The ability of TrwD to interact with lipid bilayers in the presence of millimolar concentrations of calcium ions resem-

bles the properties of annexins (7, 11), although there is no similarity in the conserved residues of the two protein families (our unpublished observations).

The above-described experiments with model membranes do not actually demonstrate that TrwD causes membrane aggregation and/or fusion as part of its normal function but rather point to its general capacity to bind and perturb cell membranes under a variety of conditions. TrwD is the first known protein that is essential for conjugation and perturbs the membrane structure. In the light of the above results, we propose that TrwD interacts with the membranous systems to build up the transport assemblage that facilitates DNA transfer. Namely, the hollow interior of the hexamer might be the receptacle for a chaperone-like activity related to the folding, or membrane delivery, of one or more of the components that form the DNA transport conduit. The other properties of TrwD, i.e., ATPase activity, possible interaction with other macromolecules, and membership in a large protein family, also locate this protein at a pivotal position in the bacterial conjugation and macromolecular transfer phenomena.

REFERENCES

1. **Alonso, A., A. Villena, and F. M. Goñi.** 1981. Lysis and reassembly of sonicated lecithin vesicles in the presence of Triton X-100. FEBS Lett. **123:**200–204.
2. **Altschul, S. F., T. L. Madden, A. A. Schäffer, J. Zhang, Z. Zhang, W. Miller, and D. J. Lipman.** 1997. Gapped BLAST and PSI-BLAST: a new generation of protein database search programs. Nucleic Acids Res. **25:**3389–3402.
3. **Bakás, L., H. Ostolaza, W. L. C. Vaz, and F. M. Goñi.** 1996. Reversible adsorption and nonreversible insertion of *Escherichia coli* α-haemolysin in phospholipid bilayers. Biophys. J. **71:**1869–1876.
4. **Basáñez, G., J. L. Nieva, F. M. Goñi, and A. Alonso.** 1996. Origin of the lag period in the phospholipase C cleavage of phospholipids in membranes. Biochemistry **35:**15183–15187.
5. **Benachir, T., and M. Lafleur.** 1995. Study of vesicle leakage induced by melittin. Biochim. Biophys. Acta **1235:**452–460.
6. **Bentz, J., S. Nir, and D. G Covell..** 1988. Mass action kinetics of virus-cell aggregation and fusion. Biophys. J. **54:**449–462.
7. **Bitto, E., and W. Cho.** 1999. Structural determinant of the vesicle aggregation activity of annexin I. Biochemistry **38:**14094–14100.
8. **Bolland, S., M. Llosa, P. Avila, and F. de la Cruz.** 1990. General organization of the conjugal transfer genes of the IncW plasmid R388 and interactions between R388 and IncN and IncP plasmids. J. Bacteriol. **172:**5795–5802.
9. **Caaveiro, J. M. M., A. Molina, P. Rodríguez-Palenzuela, F. M. Goñi, and J. M. González-Mañas.** 1998. Interaction of wheat alpha-thionin with large unilamellar vesicles. Protein Sci. **7:**2567–2577.
10. **Chernomordik, L., A. Chanturiya, and J. Green.** 1995. The hemifusion intermediate and its conversion to complete fusion. Regulation by lipid composition. Biophys. J. **69:**922–929.
11. **Creutz, C. E.** 1992. The annexins and exocytosis. Science **258:**924–931.
12. **de la Cruz, F., and E. Lanka.** 1998. Function of the Ti-plasmid Vir proteins: T-complex formation and transfer to the plant cell, p. 281–301. *In* H. P. Spaink, A. Kondorosi, and P. J. J. Hooykaas (ed.), The *Rhizobiaceae*. Kluwer Academic Publishers, Hingham, Mass.
13. **Dibble, A. R., M. D. Yeager, and G. W. Feigenson.** 1993. Partitioning of gramicidin A between coexisting fluid and gel phospholipid phases. Biochim. Biophys. Acta **1153:**155–162.
14. **Edwards, K., and M. Almgren.** 1991. Solubilization of lecithin vesicles by C12E8. J. Colloid Interface Sci.**147:**1–21.
15. **Ellens, H., J. Bentz, and F. C. Szoka.** 1985. H⁺- and Ca²⁺-induced fusion and destabilization of liposomes. Biochemistry **24:**3099–3106.
16. **Gershfeld, N. L.** 1978. Equilibrium studies of lecithin-cholesterol interactions. Biophys. J. **22:**469–488.
17. **Goldberg, E. M., D. S. Lester, D. B. Borchardt, and R. Zidovetzki.** 1994.

Effects of diacylglycerol and Ca^{2+} on structure of phosphatidylcholine/phosphatidylserine bilayers. Biophys. J. **66:**382–393.

18. **Goñi, F. M., G. Basáñez, M. B. Ruiz-Argüello, and A. Alonso.** 1998. Interfacial enzyme activation, non-lamellar phase formation and membrane fusion. Is there a conducting thread? Faraday Discuss. **111:**55–68.

19. **Hobbs, M., and J. S. Mattick.** 1993. Common components in the assembly of type IV fimbriae, DNA transfer systems, filamentous phage and protein-secretion apparatus. Mol. Microbiol. **10:**233–243.

20. **Hoekstra, D., T. de Boer, K. Klappe, and J. Wilschut.** 1984. Fluorescence method for measuring the kinetics of fusion between biological membranes. Biochemistry **23:**5675–5681.

21. **Krause, S., M. Bárcena, W. Pansegrau, R. Lurz, J. M. Carazo, and E. Lanka.** 2000. Sequence-related protein export NTPases encoded by the conjugative transfer region of RP4 and by the *cag* pathogenicity island of *Helicobacter pylori* share similar hexameric ring structures. Proc. Natl. Acad. Sci. USA **97:**3067–3072.

22. **Krause, S., W. Pansegrau, R. Lurz, F. de la Cruz, and E. Lanka.** 2000. Enzymology of type IV macromolecule secretion systems: the conjugative transfer regions of plasmids RP4 and R388 and the *cag* pathogenicity island of *Helicobacter pylori* encode structurally and functionally related NTP-hydrolases. J. Bacteriol. **182:**2761–2770.

23. **Matsuzaki, K.** 1998. Magainins as paradigm for the mode of action of pore forming polypeptides. Biochim. Biophys. Acta **1376:**391–400.

24. **Mayer, L. D., M. J. Hope, and P. R. Cullis.** 1986. Vesicles of variable sizes produced by a rapid extrusion procedure. Biochim. Biophys. Acta **858:**161–168.

25. **McIntyre, J. C., and R. G. Sleight.** 1991. Fluorescence assay for phospholipid membrane asymmetry. Biochemistry **30:**11819–11827.

26. **Morero, R. D., A. L. Viñals, B. Bloj, and R. N. Farias.** 1985. Fusion of phospholipid vesicles induced by muscle glyceraldehydes-3-phosphate dehydrogenase in the absence of calcium. Biochemistry **24:**1904–1909.

27. **Nicolay, K., R. van der Neut, J. J. Fok, and B. de Kruijff.** 1985. Effects of adriamycin on lipid polymorphism in cardiolipin containing model and mitochondrial membranes. Biochim. Biophys. Acta **819:**55–65.

28. **Nieva, J. L., F. M. Goñi, and A. Alonso.** 1989. Liposome fusion catalytically induced by phospholipase C. Biochemistry **28:**7364–7367.

29. **Nir, S., and J. L. Nieva.** 2000. Interactions of peptides with liposomes: pore formation and fusion. Prog. Lipid Res. **39:**181–206.

30. **Parente, R. A., S. Nir, and F. C. Szoka.** 1990. Mechanism of leakage of phospholipid vesicle contents induced by the peptide GALA. Biochemistry **29:**8720–8728.

31. **Pereira, F. B., F. M. Goñi, and J. L. Nieva.** 1995. Liposome destabilization induced by the HIV-1 fusion peptide. Effect of a single amino acid substitution. FEBS Lett. **362:**243–246.

32. **Pereira, F. B., F. M. Goñi, A. Muga, J. L. Nieva.** 1997. Permeabilization and

33. **Planet, P. J., S. C. Kachlany, R. DeSalle, and D. H. Figurski.** 2001. Phylogeny of genes for secretion NTPases: identification of the widespread *tad*A subfamily and development of a diagnostic key for gene classification. Proc. Natl. Acad. Sci. USA **98:**2503–2508.

34. **Possot, E., C. d'Enfert, I. Reyss, and A. Pugsley.** 1992. Pullulanase secretion in *Escherichia coli* K-12 requires a cytoplasmic protein and a putative polytopic cytoplasmic protein. Mol. Microbiol. **6:**95–105.

35. **Rivas, S., S. Bolland, E. Cabezón, F. M. Goñi, and F. de la Cruz.** 1997. TrwD, a protein encoded by the IncW plasmid R388, displays an ATPase activity essential for bacterial conjugation. J. Biol. Chem. **272:**25583–25590.

36. **Rost, B., and C. Sander.** 1993. Improved prediction of protein secondary structure by use of sequence profiles and neural networks. Proc. Natl. Acad. Sci. USA **90:**7558–7562.

37. **Soloaga, A., M. P. Veiga, L. M. García-Segura, H. Ostolaza, R. Brasseur, and F. M. Goñi.** 1999. Insertion of *Escherichia coli* alpha-haemolysin in lipid bilayers as a non-transmembrane integral protein. Mol. Microbiol. **31:**1013–1024.

38. **Stegmann, T., P. Schoen, R. Bron, J. Wey, I. Bartoldus, A. Ortiz, J. L. Nieva, and J. Wilschut.** 1993. Evaluation of viral membrane fusion assays. Comparison of the octadecylrhodamine quenching assay with the pyrene excimer assay. Biochemistry **32:**11330–11337.

39. **Stephens, K. M., C. Roush, and E. Nester.** 1995. *Agrobacterium tumefaciens* VirB11 protein requires a consensus nucleotide-binding site for function in virulence. J. Bacteriol. **177:**27–36.

40. **Struck, D. K., D. Hoekstra, and R. E. Pagano.** 1981. Use of resonance energy transfer to monitor membrane fusion. Biochemistry **20:**4093–4099.

41. **Viguera, A. R., M. Mencía, and F. M. Goñi.** 1993. Time-resolved and equilibrium studies of the effects of poly(ethylene glycol) on small unilamellar phospholipid vesicles. Biochemistry **32:**3708–3713.

42. **Wilschut, J., M. Holsappel, and R. Jansen.** 1982. Ca^{2+}-induced fusion of cardiolipin/phosphatidylcholine vesicles monitored by mixing of aqueous contents. Biochim. Biophys. Acta **690:**297–301.

43. **Wilschut, J., S. Nir, J. Scholoma, and D. Hoekstra.** 1985. Kinetics of Ca^{2+}-induced fusion of cardiolipin/PC vesicle: correlation between vesicle aggregation, bilayer destabilization and fusion. Biochemistry **24:**4630–4636.

44. **Yeo, H. J., S. N. Savvides, A. B. Herr, E. Lanka, and G. Waksman.** 2000. Crystal structure of the hexameric traffic ATPase of the *Helicobacter pylori* type IV secretion system. Mol. Cell **6:**1461–1472.

45. **Zechner, E. L., F. de la Cruz, R. Eisenbrandt, A. M. Grahn, G. Koraimann, E. Lanka, G. Muth, W. Pansegrau, C. M. Thomas, B. M. Wilkins, and M. Zatyka.** 2000. Conjugative-DNA transfer processes, p. 87–174. *In* C. M. Thomas (ed.), The horizontal gene pool. Bacterial plasmids and gene spread. Harwood Academic Publishers, Amsterdam, The Netherlands.